CrossMark

ORIGINAL ARTICLE

Edge-Centered DTI Connectivity Analysis: Application to Schizophrenia

Edward H. Herskovits[1] · L. Elliot Hong[2] · Peter Kochunov[2] ·
Hemalatha Sampath[2] · Rong Chen[1]

Abstract Diffusion tensor imaging (DTI) provides connectivity information that helps illuminate the processes underlying normal development as well as brain disorders such as autism and schizophrenia. Researchers have widely adopted graph representations to model DTI connectivity among brain structures; however, most measures of connectivity have been centered on nodes, rather than edges, in these graphs. We present an edge-based algorithm for assessing anatomic connectivity; this approach provides information about connections among brain structures, rather than information about structures themselves. This perspective allows us to formulate multivariate graph-based models of altered connectivity that distinguish among experimental groups. We demonstrate the utility of this approach by analyzing data from an ongoing study of schizophrenia.

Keywords Diffusion tensor imaging · Network analysis · Tractography · Schizophrenia · Data mining

Introduction

Although magnetic resonance (MR) examination has provided invaluable anatomic information about the structure of the human brain, researchers have recognized that signal-intensity and morphological changes cannot provide a complete picture of neurological and psychiatric disorders. Investigations of psychiatric disorders, brain development, and epilepsy stand to benefit immensely from noninvasive delineation of connectivity. Basic and clinical neuroscience researchers have widely adopted diffusion tensor imaging (DTI) to delineate anatomic connectivity, in a broad range of settings, including brain development (Cascio et al. 2007; Dubois et al. 2006; Eluvathingal et al. 2007; Hagmann et al. 2010; Hüppi and Dubois 2006; Kasprian et al. 2008), aging (Makris et al. 2007; Ystad et al. 2011), epilepsy (Liao et al. 2011), multiple sclerosis (Testaverde et al. 2012), and psychiatric and behavioral disorders (Ayling et al. 2012; Sexton et al. 2009; Travers et al. 2012; Wang et al. 2012; White et al. 2008). Recognizing the importance of DTI, functional MR and other modalities in constructing connectivity models of the human brain, the NIH has initiated the Human Connectome Project, the goal of which is to "acquire and share data about the structural and functional connectivity of the human brain" (NIH 2013).

Most DTI analyses do not directly compare connectivity (i.e., the presence or strengths of connections) across experimental groups. One of the most common forms of DTI analysis is tract-based spatial statistics (TBSS), which was developed by Smith et al. (Smith et al. 2006). In this approach, DTI data (e.g., voxel-wise fractional anisotropy [FA] values) are registered to a skeletonized mean FA image, which is created from a preliminary registration of all subjects' FA volumes; voxel-wise statistics, such as multiple regression, are then computed across the common FA skeleton. As with other voxel-wise approaches, TBSS suffers from the multiple-comparison problem, which the authors advise to ameliorate via a permutation-based approach (e.g., (Nichols and Holmes 2002)). An additional problem with voxel-wise analyses, as currently performed, is that these algorithms are typically applied to signal-intensity (e.g., FA) values, rather than to connectivity patterns; although changes in FA values imply

✉ Edward H. Herskovits
ehh@ieee.org

[1] Department of Diagnostic Radiology and Nuclear Medicine, University of Maryland, Baltimore, MD, USA

[2] Maryland Psychiatric Research Center, Department of Psychiatry, University of Maryland, Baltimore, MD, USA

 Springer

altered connectivity, researchers have yet to elucidate the relationship between DTI-derived scalar values and connectivity.

The major alternative to mass-univariate voxel-wise analysis of scalar DTI metrics is tractography. As described by Toga et al. (2012), tractography consists of two major steps: voxel-wise estimation of a diffusion vector, and deterministic or probabilistic estimation of fibers across voxels (i.e., fiber tracking). This process yields a (strictly triangular) connectivity matrix (CM), in which entries quantify connectivity strength between two brain regions. CM comparison across experimental groups, or over time, has the potential to delineate detailed differences in connectivity. The principal challenges inherent to comparing CMs are threefold: undersampling; reliance on structure-centered, rather than connection-centered, statistics; and reliance on mass-univariate statistics.

Graph theory offers a natural means for describing connectivity patterns, in that nodes and edges represent brain structures and connections among them, respectively; there is a one-to-one mapping between a CM and an undirected graph. A rapidly growing group of neuroscientists, computer scientists and mathematicians have investigated graph-theoretical approaches to modeling brain networks (He and Evans 2010). Researchers have used this framework to compare topological properties of these network graphs, such as modularity, characteristic path length, and communicability (Bullmore and Sporns 2009; Crofts and Higham 2009; Watts and Strogatz 1998). For example, the small-world property describes a network that consists of sparsely connected cliques (highly interconnected groups of nodes), in contrast to lattices—which are uniformly connected—and randomly connected networks.

Although this approach has clearly demonstrated its utility, it suffers from two principal limitations. First, graph-theoretical metrics measure properties of nodes, rather than of edges. For example, although a change in efficiency may indicate an important change in connectivity for a brain structure **S**, it does not directly indicate the other structures that have gained or lost connections to **S**. Second, these metrics have no formal foundation; the choice of which network metrics to compute in a given analysis has no grounding in first principles, and conclusions based on various metrics may differ.

More recently, Zalesky et al. have proposed a network-based statistic (NBS) to ameliorate the multiple-comparison problem for graph-theoretical metrics (Zalesky et al. 2010). Instead of computing connection-wise probabilities, they propose computing p-values for network-based graph-theoretical metrics. Toward this end, they apply permutation testing and connection-wise significance thresholds to generate a network for which they compute a NBS; of note, they determine these significance thresholds empirically. In essence, under this approach networks are equivalent to the clusters that are detected using statistical parametric mapping. They demonstrated that a network-based approach results in fewer false positive results, at the cost of loss of information about pair-wise connectivity.

We herein investigate the utility of discrete Bayesian multivariate analysis of connectivity matrices. Although we also use graphs to model brain networks, our approach focuses on connections among brain structures, rather than on brain structures themselves. This difference allows us to delineate *specific* connectivity differences that distinguish experimental groups. In addition, we make extensive use of bootstrap resampling and ensemble methods to minimize overfitting that results from undersampled data. We demonstrate the utility of this approach by analyzing data from an ongoing study of schizophrenia.

Methods

Our approach for analyzing CM values consists of three steps (Fig. 1): connectivity-score computation, variable selection, and Bayesian network (BN) generation.

Subjects

We analyzed DTI data from 126 subjects: 48 individuals with schizophrenia (age=40.2±13.4 years) and 78 control subjects (age=39.8±12.9 years). All participants provided written informed consent that had been approved by the University of Maryland Internal Review Board. All participants were evaluated using the Structured Clinical Interview for the DSM-IV. We recruited subjects with an Axis I diagnosis of schizophrenia or schizoaffective disorder through the Maryland Psychiatric Research Center, and neighboring mental-health clinics. We recruited control subjects, who did not have an Axis I psychiatric diagnosis, through media advertisements. Exclusion criteria included hypertension, hyperlipidemia, type 2 diabetes, heart disorders, and major neurological events, such as stroke or transient ischemic attack. Illicit substance and alcohol abuse and dependence were exclusion criteria. Except for seven medication-free participants, schizophrenia patients were taking antipsychotic medications. We found no significant different in age and sex across group (p-value=0.88 for age based on two-sample t-test, and p-value=0.27 for sex based on Fisher's exact test).

Clinical Assessment

Psychosis in schizophrenia patients was assessed with the 20 item Brief Psychiatric Rating Scale total score (Overall and Gorham 1962), where the four positive symptom items—conceptual disorganization, suspiciousness, hallucination, and
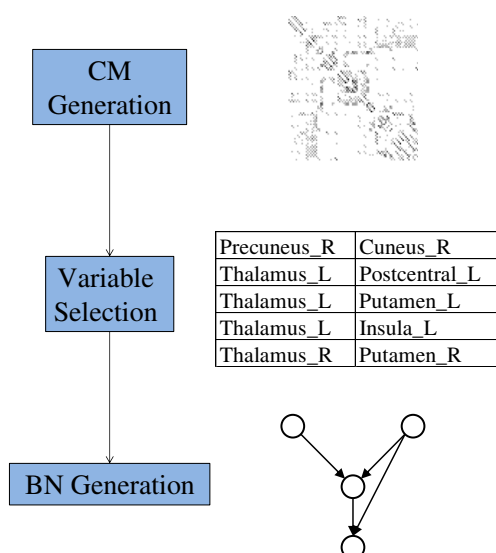
Fig. 1 Overview of the connectivity-matrix analysis algorithm

Precuneus_R	Cuneus_R
Thalamus_L	Postcentral_L
Thalamus_L	Putamen_L
Thalamus_L	Insula_L
Thalamus_R	Putamen_R

unusual thought content—were used to calculate the psychosis score. Cognitive capacities were assessed by processing speed (digit symbol coding subtest of the WAIS-III) (Wechsler 1997) and working memory (digit sequencing task) (Keefe et al. 2004). Processing speed and working memory are considered among the most robust cognitive domain deficits in schizophrenia (Dickinson et al. 2007; Knowles et al. 2010).

Diffusion Tensor Imaging (DTI)

All MR examinations were performed at the University of Maryland Center for Brain Imaging Research, using a Siemens 3-Tesla TRIO MR system (Erlangen, Germany) equipped with a 32-channel phased-array head coil. The DTI data were collected using a single-shot, echo-planar, single refocusing spin-echo, T2-weighted sequence, with GRAPPA (acceleration factor 2), yielding voxel dimensions $1.7 \times 1.7 \times 3.0$ mm, acquisition time approximately 8 min. The sequence parameters were: TE/TR=87/8, 000 ms, FOV=200 mm, axial slice orientation with 50 slices and no gap, five b=0 images and 64 isotropically distributed diffusion-weighted directions with b=700 s/mm^2. All data passed quality-assurance control of< 3 mm accumulated motion during the scan. There was no difference in average motion per TR between patients and controls (0.42 ± 0.21 mm versus 0.43 ± 0.20 mm for patients and controls, respectively). We registered image data to the AAL atlas (Tzourio-Mazoyer et al. 2002), which has 90 structures, and therefore 4,005 potential pair-wise connections.

Image Preprocessing

We processed T1-weighted MR images on a Linux workstation, running under CentOS 6.6, as follows. First, we applied the brain extraction tool (Smith 2002), which is a component of the FMRIB Software Library (FSL- RRID:birnlex_2067) (Jenkinson et al. 2012), to remove non-brain structures in both T1-weighted and DTI volumes; we used typical settings as described in (Soares et al. 2013). We then used FSL's FAST algorithm for tissue segmentation. We next registered each subject's T1-weighted image to the Montreal Neurological Institute (MNI) space, using FSL's nonlinear registration algorithm. Based on the generated deformation field, we parcellated each individual brain into 90 structures defined in the AAL (RRID:nlx_157677) template.

Similarly, we used an FSL-based pipeline to process DTI data in a manner similar to (Korgaonkar et al. 2012). First, we corrected the DTI data for head movement and eddy-current distortion. We then fitted a diffusion tensor model at each voxel. For each subject, we used the transformation from structural to diffusion space generated by FSL FDT registration to register the labeled brain regions obtained by T1 MR parcellation to that subject's DTI space; this step yielded a brain parcellation defined in that subject's DTI space.

Connectivity-score Computation

For a connectivity network of N brain structures, the corresponding CM has $N(N-1)/2$ connection-strength entries. For two distinct brain structures p and q, let $C(p, q)$ denote the connectivity score for the connection between p and q. Our procedure to generate $C(p, q)$ is as follows. 1) Based on the results of FSL probabilistic fiber-tracking (Behrens et al. 2007) with 500 seeds / white-matter voxel (after (Buchanan et al. 2014)), count the number of samples starting with white-matter voxels in brain region p and passing through brain region q. 2) Normalize this quantity (i.e., the streamline number) by the volume of region p, thereby generating the CM entries. 3) Replace $C(p, q)$ and $C(q, p)$ by the average of these two quantities, to enforce symmetry with respect to connectivity; the CM thus becomes upper-triangular. 4) Determine a threshold T such that, if we treat all $C(p, q)$ values below this threshold as not connected (i.e., if $C(p, q) < T$, $C(p, q) \leftarrow 0$), we obtain a network with connection density=0.3, which has been observed to be a lower limit for primate brain networks (Felleman and Van Essen 1991; Sporns 2011). We apply this threshold, and refer to the resulting $C(p, q)$ as a connectivity score.

Variable Selection

We use bootstrap resampling for variable selection, i.e., to detect connections that distinguish among experimental

groups. Each resampling iteration k yields a perturbed version of the original data set D, designated as D_k. Then, for D_k, we compute Wilcoxon statistics and apply a false-discovery rate corrected p-value threshold of 0.05, to determine whether any connections differ across experimental groups. Let B_k denote the set of connections demonstrating significant group differences for D_k, and let K denote the total number of iterations. We aggregate $B_1, B_2, \ldots, B_K$ to form a model ensemble, and calculate the frequency of occurrence of each connection E, defined as $f(E) = (\sum_k I[E \in B_k])/K$, where $I[condition]=1$ if $condition$ is true, otherwise 0. If $f(E) > 0.8$, that is, if connection E was detected in at least 80 % of resampled data sets, we select E as a biomarker.

Bayesian-Network Generation

To apply discrete BNs to the selected edges, we must define a threshold to label each edge as manifesting normal or decreased connectivity. Toward this end, we generated BN ensembles (see next paragraph) across a range of connectivity discretization thresholds, and found that the median of the NC group (which has lower variance than the SZ group) yielded a local minimum in the size of the resulting ensemble, and the size of the Markov blanket for the group-membership variable G, which should prevent over-fitting. Accordingly, we define the indicator connectivity variable $BC(p, q)$ as 'decreased connectivity' if $C(p, q)$ is less than the median of the NC group; otherwise, we define $BC(p, q)$ as 'normal connectivity'. The set of binary variables $BC(p, q)$ characterizes each subject's connectivity profile.

Given a set of binary connectivity profiles for all subjects, we can apply standard BN-generation algorithms to determine multivariate combinations of connectivity patterns that distinguish among experimental groups. In addition, we again employ bootstrap resampling to these data to prevent over-fitting. We constrain BN structures to place the group-membership variable G as a leaf node in BNs; that is, G may have parent nodes, but may not have child nodes. In this manner, we assess the extent to which connectivity patterns affect G, rather than assessing the effects of G on connectivity patterns. During the kth bootstrap iteration, we identify the Markov blanket (i.e., parent set) of G in BN_k, and denote this set of variables as MB_k. We identify the most probable network resulting from resampling as BN_{max}, and the probability of this network as P_{max}. We then consider all networks generated by resampling; based on the Bayes factor literature (e.g., (Kass and Raftery 1995), we select only those networks with probability greater than $0.1 \times P_{max}$ when generating a Markov-blanket ensemble. We then use the resulting ensemble to calculate the frequency of each connection, in a manner similar to that described in the preceding section.

Experimental Results

Variable Selection

We employed bootstrap resampling with $K=2,000$, and frequency threshold of 0.8; this process yielded 15 connections (Table 1) that could potentially distinguish between the NC and SZ groups. All of these connections manifested decreased connectivity in the SZ group, relative to the NC group. Note the prominence of decreased interhemispheric connectivity,

Table 1 Connections that differed between groups in at least 80 % of bootstrap samples. Connectivity strength is in arbitrary units. NC = control subject, SZ = schizophrenia subject

Connection structure names		Median connectivity		Wilcoxon p-value (x 10^{-5})
Cingulum_Mid_R	Cingulum_Ant_L	7.77	4.73	1.31
Precuneus_R	Cuneus_R	90.21	73.93	2.53
Precuneus_L	Cingulum_Mid_R	6.64	3.58	2.73
Postcentral_R	Frontal_Inf_Oper_R	4.15	1.83	2.79
Temporal_Mid_L	Frontal_Inf_Tri_L	5.21	2.05	4.01
Thalamus_L	Postcentral_L	16.31	7.92	4.57
Paracentral_Lobule_R	Cingulum_Mid_L	7.32	3.71	5.19
Cingulum_Mid_R	Cingulum_Mid_L	21.52	12.26	5.91
Thalamus_L	Parietal_Sup_L	13.29	7.73	6.30
Thalamus_R	Putamen_R	25.92	14.68	9.00
Thalamus_R	Rolandic_Oper_R	4.05	1.97	13.15
Thalamus_L	Rolandic_Oper_L	2.87	1.40	14.37
Thalamus_L	Putamen_L	69.54	54.30	15.66
Thalamus_L	Insula_L	7.16	3.79	19.72
Temporal_Mid_R	Temporal_Sup_R	63.67	53.78	20.32

Table 2 The four most probable parent sets resulting from bootstrap resampling with 2,000 iterations. We selected the parent sets for BNs with probabilities that were within a factor of 10 of the most probable model (i.e., parent sets from BNs 1–3) to generate SVM classification models.

For reference, note that the BN with no parents was never generated in 2,000 trials. NC/SZ = control or schizophrenia subject (class-membership variable)

Rank	Parents of NC/SZ		BDe Score	Bayes Factor
N/A	None		−86.38	0.000074
1	Cingulum_Mid_R	Cingulum_Ant_L	−76.86	1
	Paracentral_Lobule_R	Cingulum_Mid_L		
2	Cingulum_Mid_R	Cingulum_Ant_L	−78.58	0.18
	Postcentral_R	Frontal_Inf_Oper_R		
3	Cingulum_Mid_R	Cingulum_Ant_L	−79.02	0.12
	Temporal_Mid_L	Frontal_Inf_Tri_L		
	Paracentral_Lobule_R	Cingulum_Mid_L		
4	Cingulum_Mid_R	Cingulum_Ant_L	−79.43	0.08
	Temporal_Mid_L	Frontal_Inf_Tri_L		

and extensive decreased connectivity of both thalami, in the SZ group.

Bayesian-Network Generation

We applied a connectivity-strength threshold based on the median of the NC group, to all $C(p, q)$ in Table 1, thereby obtaining 15 binary variables. We then employed greedy search and the BDe metric (Heckerman et al. 1995) as implemented in the R package bnlearn (Scutari 2009), and bootstrap resampling with 2,000 iterations, to generate the Markov blanket ensemble shown in Table 2. Selecting those BNs with Bayes factor > 0.10 (relative to P_{max}), we obtained the 3 BNs shown in Fig. 2, and box plots for each of these variables in Fig. 3. Note the high variability shown in box plots of the four features, which is expected, given undersampling.

Table 3 shows the conditional-probability tables corresponding to the networks in Fig. 2. Examination of these tables provides insight beyond that obtained from the corresponding network structures. For example, the conditional probabilities in Table 3 indicate that, of subjects with normal left fronto-temporal connectivity (even-numbered rows), those that have either normal right-frontal or interhemispheric connectivity are very unlikely to have

schizophrenia, whereas Table 3 indicates that those with decreased right-frontal and interhemispheric connectivity are more likely than not to have schizophrenia. Similarly, extensively decreased interhemispheric connectivity, as manifest in CMR-CAL and PLR-CML (rows 1–2), is highly characteristic of schizophrenia subjects; the inverse is also true (rows 7–8).

For comparison, we generated a BN directly from the 126 samples of 15 binary connectivity variables, without resampling. Figure 4 shows this network, which contains the same three variables found in BNs generated by resampling techniques. We can apply standard BN inference algorithms (Huang and Darwiche 1996) to answer arbitrary queries of the variables in this BN. For example, with no evidence, we obtain the prior probability distribution over all variables (e.g., P(NC)=0.68). If we set G=SZ and CMR-CAL=Normal, we find that P(PLR-CML=Normal | G=SZ, CMR-CAL=Normal)=0.77.

Validation

We employed two methods for validating the connectivity variables that we detected for these data: cross validation, and correlation with clinical assessment.
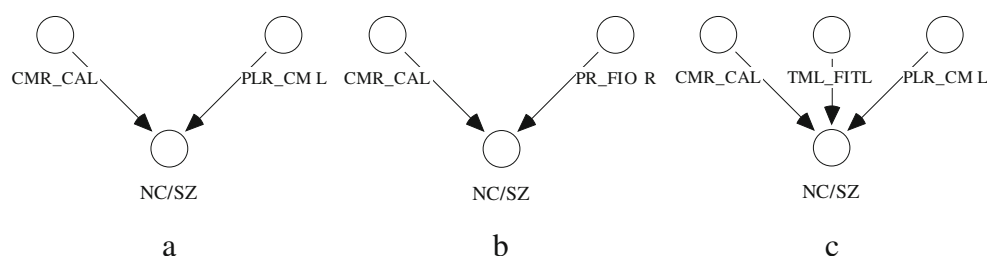

Fig. 2 The top 3 BNs generated by bootstrap resampling (see Table 2). CMR-CAL = Cingulum_Mid_R - Cingulum_Ant_L; PLR-CML = Paracentral_Lobule_R - Cingulum_Mid_L; PR-FIOR = Postcentral_R - Frontal_Inf_Oper_R; TML-FITL = Temporal_Mid_L - Frontal_Inf_Tri_L; NC/SZ = control or schizophrenia subject (class-membership variable)

Fig. 3 Box plots of connectivity strength (arbitrary units) for the 4 variables in the BNs in Fig. 2. CMR-CAL = Cingulum_Mid_R - Cingulum_Ant_L; PLR-CML = Paracentral_Lobule_R - Cingulum_Mid_L; PR-FIOR = Postcentral_R - Frontal_Inf_Oper_R; TML-FITL = Temporal_Mid_L - Frontal_Inf_Tri_L
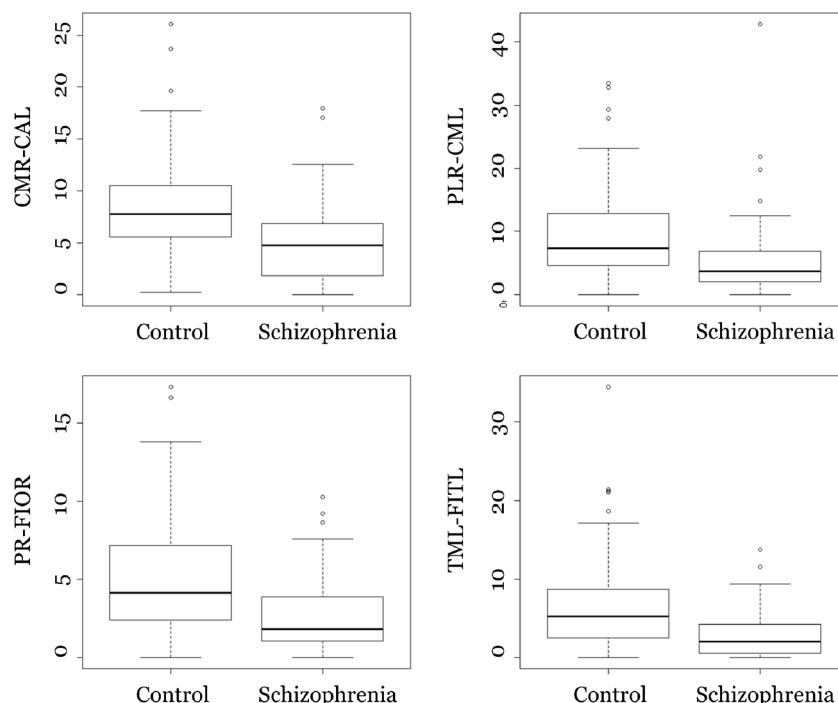

Table 3 Conditional-probability tables (and counts) corresponding to the BNs shown in Fig. 2. CMR-CAL = Cingulum_Mid_R - Cingulum_Ant_L; PLR-CML = Paracentral_Lobule_R - Cingulum_Mid_L; PR-FIOR = Postcentral_R - Frontal_Inf_Oper_R; TML-FITL = Temporal_Mid_L - Frontal_Inf_Tri_L. NC = control subject, SZ = schizophrenia subject

a

CMR-CAL	PLR-CML	P(NC)	P(SZ)
Decreased	Decreased	0.34 (18)	0.66 (35)
Decreased	Normal	0.78 (21)	0.22 (6)
Normal	Decreased	0.95 (21)	0.05 (1)
Normal	Normal	0.75 (18)	0.25 (6)

b

CMR-CAL	PR-FIOR	P(NC)	P(SZ)
Decreased	Decreased	0.31 (15)	0.69 (33)
Decreased	Normal	0.75 (24)	0.25 (8)
Normal	Decreased	0.83 (24)	0.17 (5)
Normal	Normal	0.88 (15)	0.12 (2)

c

CMR-CAL	PLR-CML	TML-FITL	P(NC)	P(SZ)
Decreased	Decreased	Decreased	0.26 (10)	0.74 (29)
Decreased	Decreased	Normal	0.57 (8)	0.43 (6)
Decreased	Normal	Decreased	0.60 (9)	0.40 (6)
Decreased	Normal	Normal	1.00 (12)	0.00 (0)
Normal	Decreased	Decreased	0.92 (11)	0.08 (1)
Normal	Decreased	Normal	1.00 (10)	0.00 (0)
Normal	Normal	Decreased	0.69 (9)	0.31 (4)
Normal	Normal	Normal	0.82 (9)	0.18 (2)

Cross Validation

First, we used these 4 variables without thresholding to construct several support vector machine (SVM) models, and then performed 10-fold cross validation of these models. Table 4 indicates that classification accuracies for models including 2 or 3 connectivity variables were greater than those for either variable alone, indicating that connectivity patterns that distinguish NC from SZ are better represented by multivariate than by univariate models.

Correlation with Clinical Assessment

As an independent source of validation, we sought to determine whether these connectivity variables were associated with clinical manifestations of schizophrenia. Toward this
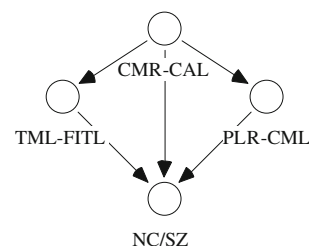

Fig. 4 The BN generated without resampling, based on the 15 binary variables listed in Table 1. CMR-CAL = Cingulum_Mid_R - Cingulum_Ant_L; PLR-CML = Paracentral_Lobule_R - Cingulum_Mid_L; TML-FITL = Temporal_Mid_L - Frontal_Inf_Tri_L; NC/SZ = control or schizophrenia subject (class-membership variable)

Table 4 Cross-validation classification accuracies for SVM models based on the 4 variables in Fig. 2. CMR-CAL = Cingulum_Mid_R - Cingulum_Ant_L; PLR-CML = Paracentral_Lobule_R - Cingulum_Mid_L; PR-FIOR = Postcentral_R - Frontal_Inf_Oper_R; TML-FITL = Temporal_Mid_L - Frontal_Inf_Tri_L

Model	Prediction Accuracy
CMR-CAL	0.65
TML-FITL	0.61
PR-FIOR	0.62
PLR-CML	0.62
CMR-CAL + PLR-CML	0.72
CMR-CAL + PR-FIOR	0.76
CMR-CAL + TML-FITL + PLR-CML	0.75

end, we computed Spearman correlation statistics with the following clinical variables: working memory, processing speed, and psychosis; the first two variables were assessed for all subjects, whereas the psychosis score was assessed for schizophrenia subjects only. As shown in Table 5, working memory was strongly correlated with interhemispheric and left fronto-temporal connectivity, and processing speed was strongly correlated with interhemispheric connectivity. Within the schizophrenia group, the psychosis score may be correlated with left fronto-temporal and right-frontal connectivity, but these correlations did not survive Bonferroni correction.

Discussion

CM-based analysis offers a complementary approach to other graph-based connectivity analyses. Whereas the latter offer measures of node connectivity, CM-based analysis is edge-centered, and allows the assessment of relative connection strengths across experimental groups, thereby providing information regarding particular tracts that may be affected in neurological or psychiatric disorders.

Our approach, being based on a discrete BN representation, has important strengths and weaknesses relative to other

Table 5 Spearman correlation p-values for the 4 variables in Fig. 2, with respect to clinical-assessment variables. Working memory and processing speed were assessed for all subjects, whereas psychosis was assessed for schizophrenia subjects only. CMR-CAL = Cingulum_Mid_R - Cingulum_Ant_L; PLR-CML = Paracentral_Lobule_R - Cingulum_Mid_L; PR-FIOR = Postcentral_R - Frontal_Inf_Oper_R; TML-FITL = Temporal_Mid_L - Frontal_Inf_Tri_L

Variable	CMR-CAL	TML-FITL	PR-FIOR	PLR-CML
Working memory	0.003	<0.001	0.125	<0.001
Processing speed	<0.001	0.017	0.224	<0.001
Psychosis (SZ)	0.263	0.023	0.042	0.112

approaches to connectivity analysis. We chose to base our approach on the discrete, rather than continuous, BN model, because discrete BNs can represent any distribution over categorical variables (Pearl 1988), whereas continuous BNs are restricted to multivariate Gaussian distributions. Discrete BNs provide several sources of connectivity information: the structure of the BN provides immediate visual feedback regarding important connections in distinguishing among experimental groups, the conditional probabilities, and, more generally, BN inference algorithms, allow researchers to determine in detail how connectivity, group-membership, and other variables incorporated into the BN model interact. However, this expressive power comes at the cost of having to select thresholds for continuous variables, such as the connectivity metric $C(p, q)$. Selecting a threshold can be difficult, as the result of subsequent analysis will clearly differ as one varies a threshold across its range. Although we found that varying the $C(p, q)$ threshold yielded a local minimum of ensemble size and of Markov blanket size at approximately the median of the NC group, it may be the case that for some applications, such preliminary analyses yield no clear threshold, in which case a discrete BN model may not be appropriate. In addition, the number of conditional probabilities will, in the worst case, increase exponentially in the number of variables. Some conditional probabilities, such as a few in Table 3, may be based on low cell counts, and will therefore have relatively high variance; in the case of the analyses reported here, the connectivity models we obtained corresponded well with results reported in the literature, indicating that resampling techniques and adequate cell counts in other cells at least partially ameliorate undersampling.

Our results confirm reports in the psychiatry literature of consistent connectivity differences between schizophrenics and control subjects (Fornito et al. 2012; Konrad and Winterer 2008). All 15 connectivity measures that resulted from variable selection were decreased in schizophrenics relative to control subjects, which is consistent with the literature. Our analysis indicates that local connectivity in the left fronto-temporal and right frontal regions, as well as interhemispheric connectivity, is decreased in schizophrenics.

Given the high variability in each individual connectivity feature, we would expect that a combination of features would more accurately classify subjects than would the best single feature. We found this to be the case: models with two or three variables yielded more accurate SVM classifiers than the best model based on a single variable. Despite the high variability in feature values, we found that a small set of features was consistently seen in models obtained by various model-generation techniques. In particular, of the 15 candidate variables in Table 1, combinations of CMR-CAL, PLR-CML, PR-FIOR, and TML-FITL were present in all models resulting from CM analysis. Therefore, it is highly likely that there are

systematic anatomic-connectivity differences between these two groups of subjects.

Both cross-validation and clinical-correlation results indicate the validity of the four connections we obtained from BN-based analysis. Validation based on clinical variables, which were not used to generate any of the BN models, yielded particularly interesting results. The association between inter-hemispheric connectivity and working memory has been reported in schizophrenia (Wheeler et al. 2014). Similarly, disrupted fronto-temporal functional connectivity has been reported in schizophrenics with impaired working memory (Fletcher et al. 1999; Meyer-Lindenberg et al. 2001), and disrupted fronto-temporal connectivity has been demonstrated in patients with first-episode psychosis (Crossley et al. 2009).

Overall, the results we have reported provide four perspectives on anatomic connectivity. First, the results of variable selection, i.e., the list of edges that differ significantly between groups, summarize differential connectivity patterns. Second, the multivariate BN model ensemble identifies that subset of connection patterns that render the group-membership variable conditionally independent of all other connectivity variables: once the states of these core variables are known, no other connectivity information will influence classification. Third, examination of the ensemble BNs' conditional-probability tables reveals particular connectivity patterns that are characteristic of various subsets of subjects; this information may find applications in characterizing subgroups of complex disorders, such as schizophrenia and autism. Finally, freely available BN inference algorithms allow researchers to perform arbitrary queries on connectivity and group-membership variables and determine virtually instantaneously the posterior distributions of the remaining variables.

To extend the utility of this approach, we plan to re-implement this analysis as a single pipeline, which will take as input DTI data, group-membership, and clinical variables, and will allow users to select an atlas, and to select or vary thresholds from default values determined by preliminary re-sampling of the data. In addition, we plan to implement a version of this analysis that exploits the inherently parallel nature of our approach.

Information Sharing Statement

The software we developed for connectivity-score computation, variable selection, and Bayesian-network generation is available from the NITRC website; this package also includes a test data set.

References

Ayling, E., Aghajani, M., Fouche, J. P., & van der Wee, N. (2012). Diffusion tensor imaging in anxiety disorders. *Current Psychiatry Reports, 14,* 197–202.

Behrens, T. E. J., Berg, H. J., Jbabdi, S., Rushworth, M. F. S., & Woolrich, M. W. (2007). Probabilistic diffusion tractography with multiple fibre orientations: what can we gain? *NeuroImage, 34,* 144–155.

Buchanan, C. R., Pernet, C. R., Gorgolewski, K. J., Storkey, A. J., & Bastin, M. E. (2014). Test-retest reliability of structural brain networks from diffusion MRI. *NeuroImage, 86,* 231–243.

Bullmore, E., & Sporns, O. (2009). Complex brain networks: graph theoretical analysis of structural and functional systems. *Nature Reviews Neuroscience, 10,* 186–198.

Cascio, C. J., Gerig, G., & Piven, J. (2007). Diffusion tensor imaging: application to the study of the developing brain. *Journal of the American Academy of Child and Adolescent Psychiatry, 46,* 213–223.

Crofts, J. J., & Higham, D. J. (2009). A weighted communicability measure applied to complex brain networks. *Journal of The Royal Society Interface, 6,* 411–414.

Crossley, N. A., Mechelli, A., Fusar-Poli, P., Broome, M. R., Matthiasson, P., Johns, L. C., et al. (2009). Superior temporal lobe dysfunction and frontotemporal dysconnectivity in subjects at risk of psychosis and in first-episode psychosis. *Human brain mapping, 30,* 4129–4137.

Dickinson, D., Ramsey, M. E., & Gold, J. M. (2007). Overlooking the obvious: a meta-analytic comparison of digit symbol coding tasks and other cognitive measures in schizophrenia. *Archives of General Psychiatry, 64,* 532–542.

Dubois, J., Hertz-Pannier, L., Dehaene-Lambertz, G., Cointepas, Y., & Le Bihan, D. (2006). Assessment of the early organization and maturation of infants' cerebral white matter fiber bundles: a feasibility study using quantitative diffusion tensor imaging and tractography. *NeuroImage, 30,* 1121–1132.

Eluvathingal, T. J., Hasan, K. M., Kramer, L., Fletcher, J. M., & Ewing-Cobbs, L. (2007). Quantitative diffusion tensor tractography of association and projection fibers in normally developing children and adolescents. *Cerebral Cortex, 17,* 2760–2768.

Felleman, D. J., & Van Essen, D. C. (1991). Distributed hierarchical processing in the primate cerebral cortex. *Cerebral Cortex, 1,* 1–47.

Fletcher, P., McKenna, P. J., Friston, K. J., Frith, C. D., & Dolan, R. J. (1999). Abnormal cingulate modulation of fronto-temporal connectivity in schizophrenia. *NeuroImage, 9,* 337–342.

Fornito, A., Zalesky, A., Pantelis, C., & Bullmore, E. T. (2012). Schizophrenia, neuroimaging and connectomics. *NeuroImage, 62,* 2296–2314.

Hagmann, P., Sporns, O., Madan, N., Cammoun, L., Pienaar, R., Wedeen, V. J., et al. (2010). White matter maturation reshapes structural connectivity in the late developing human brain. *Proceedings of the National Academy of Sciences of the United States of America, 107,* 19067–10972.

He, Y., & Evans, A. (2010). Graph theoretical modeling of brain connectivity. *Current Opinion in Neurology, 23,* 341–350.

Heckerman, D., Geiger, D., & Chickering, D. (1995). Learning Bayesian networks: the combination of knowledge and statistical data. *Machine Learning, 20,* 197–243.

Huang, C., & Darwiche, A. (1996). Inference in belief networks: a procedural guide. *International Journal of Approximate Reasoning, 15*(3), 225–263.

Hüppi, P. S., & Dubois, J. (2006). Diffusion tensor imaging of brain development. *Seminars in Fetal and Neonatal Medicine, 11,* 489–497.

Jenkinson, M., Beckmann, C. F., Behrens, T. E., Woolrich, M. W., & Smith, S. M. (2012). *FSL. NeuroImage, 62,* 782–790.

Kasprian, G., Brugger, P. C., Weber, M., Krssak, M., Krampl, E., Herold, C., & Prayer, D. (2008). In utero tractography of fetal white matter development. *NeuroImage, 43*, 213–224.

Kass, R. E., & Raftery, A. E. (1995). Bayes factors. *Journal of the American Statistical Association, 90*, 773–795.

Keefe, R. S., Goldberg, T. E., Harvey, P. D., Gold, J. M., Poe, M. P., & Coughenour, L. (2004). The brief assessment of cognition in schizophrenia: reliability, sensitivity, and comparison with a standard neurocognitive battery. *Schizophrenia Research, 68*, 283–297.

Knowles, E. E., David, A. S., & Reichenberg, A. (2010). Processing speed deficits in schizophrenia: reexamining the evidence. *American Journal of Psychiatry, 167*, 828–835.

Konrad, A., & Winterer, G. (2008). Disturbed structural connectivity in schizophrenia—primary factor in pathology or epiphenomenon? *Schizophrenia Bulletin, 34*, 72–92.

Korgaonkar, M. S., Cooper, N. J., Williams, L. M., & Grieve, S. M. (2012). Mapping inter-regional connectivity of the entire cortex to characterize major depressive disorder: a whole-brain diffusion tensor imaging tractography study. *Neuroreport, 23*, 566–571.

Liao, W., Zhang, Z., Pan, Z., Mantini, D., Ding, J., Duan, X., et al. (2011). Default mode network abnormalities in mesial temporal lobe epilepsy: a study combining fMRI and DTI. *Human Brain Mapping, 32*, 883–895.

Makris, N., Papadimitriou, G. M., van der Kouwe, A., Kennedy, D. N., Hodge, S. M., Dale, A. M., et al. (2007). Frontal connections and cognitive changes in normal aging rhesus monkeys: A DTI study. *Neurobiology of Aging, 28*, 1556–1567.

Meyer-Lindenberg, A., Poline, J.-B., Kohn, P. D., Holt, J. L., Egan, M. F., Weinberger, D. R., & Berman, K. F. (2001). Evidence for abnormal cortical functional connectivity during working memory in schizophrenia. *American Journal of Psychiatry, 158*, 1809–1817.

Nichols, T. E., & Holmes, A. P. (2002). Nonparametric permutation tests for functional neuroimaging: a primer with examples. *Human Brain Mapping, 15*, 1–25.

NIH. (2013). The NIH Blueprint for Neuroscience Research: The Human Connectome Project. http://www.neuroscienceblueprint.nih.gov/connectome.

Overall, J. E., & Gorham, D. R. (1962). The brief psychiatric rating scale. *Psychological Reports, 10*, 799–812.

Pearl, J. (1988). *Probabilistic Reasoning in Intelligent Systems: Networks of Plausible Inference*. Morgan Kaufmann.

Scutari, M. (2009). Learning Bayesian networks with the `bnlearn` R package. *arXiv preprint arXiv:0908.3817*.

Sexton, C. E., Mackay, C. E., & Ebmeier, K. P. (2009). A systematic review of diffusion tensor imaging studies in affective disorders. *Biological Psychiatry, 66*, 814–823.

Smith, S. M. (2002). Fast robust automated brain extraction. *Human Brain Mapping, 17*, 143–155.

Smith, S. M., Jenkinson, M., Johansen-Berg, H., Rueckert, D., Nichols, T. E., Mackay, C. E., et al. (2006). Tract-based spatial statistics: voxelwise analysis of multi-subject diffusion data. *NeuroImage, 31*, 1487–1505.

Soares, J. M., Marques, P., Alves, V., & Sousa, N. (2013). A hitchhiker's guide to diffusion tensor imaging. *Frontiers in Neuroscience, 7*, 31.

Sporns, O. (2011). *Networks of the brain*. Cambridge: MIT Press.

Testaverde, L., Caporali, L., Venditti, E., Grillea, G., & Colonnese, C. (2012). Diffusion tensor imaging applications in multiple sclerosis patients using 3T magnetic resonance: a preliminary study. *European Radiology, 22*, 990–997.

Toga, A. W., Clark, K. A., Thompson, P. M., Shattuck, D. W., & Van Horn, J. D. (2012). Mapping the human connectome. *Neurosurgery, 71*, 1–5.

Travers, B. G., Adluru, N., Ennis, C., Tromp, D. P. M., Destiche, D., Doran, S., et al. (2012). Diffusion tensor imaging in autism spectrum disorder: a review. *Autism Research, 5*, 289–313.

Tzourio-Mazoyer, N., Landeau, B., Papathanassiou, D., Crivello, F., Etard, O., Delcroix, N., et al. (2002). Automated anatomical labeling of activations in SPM using a macroscopic anatomical parcellation of the MNI MRI single-subject brain. *NeuroImage, 15*, 273–289.

Wang, Q., Su, T.-P., Zhou, Y., Chou, K.-H., Chen, I. Y., Jiang, T., & Lin, C.-P. (2012). Anatomical insights into disrupted small-world networks in schizophrenia. *NeuroImage, 59*, 1085–1093.

Watts, D. J., & Strogatz, S. H. (1998). Collective dynamics of "small-world" networks. *Nature, 393*, 440–442.

Wechsler, D. (1997). *Manual for the Wechsler adult intelligence scale—third edition (WAIS III)*. San Antonio, Texas: The Psychological Corporation.

Wheeler, A. L., Chakravarty, M. M., Lerch, J. P., Pipitone, J., Daskalakis, Z. J., Rajji, T. K., et al. (2014). Disrupted prefrontal interhemispheric structural coupling in schizophrenia related to working memory performance. *Schizophrenia Bulletin, 40*(4), 914–924.

White, T., Nelson, M., & Lim, K. O. (2008). Diffusion tensor imaging in psychiatric disorders. *Topics in Magnetic Resonance Imaging, 19*, 97–109.

Ystad, M., Hodneland, E., Adolfsdottir, S., Haasz, J., Lundervold, A. J., Eichele, T., & Lundervold, A. (2011). Cortico-striatal connectivity and cognition in normal aging: a combined DTI and resting state fMRI study. *NeuroImage, 55*, 24–31.

Zalesky, A., Fornito, A., & Bullmore, E. T. (2010). Network-based statistic: identifying differences in brain networks. *NeuroImage, 53*(4), 1197–1207.